Inorg. Chem. **2002**, *41*, 1816–1823

Magnetically Isolated $Cu^{II}Gd^{III}$ Pairs in the Series [Cu(acacen)Gd(pta)$_3$], [Cu(acacen)Gd(hfa)$_3$], [Cu(salen)Gd(pta)$_3$], and [Cu(salen)Gd(hfa)$_3$], [acacen = *N,N′*-Ethylenebis(acetylacetoniminate(−)), salen = *N,N′*-Ethylenebis(salicylideniminate(−)), hfa = 1,1,1,5,5,5-Hexafluoropentane-2,4-dionate(−), pta = 1,1,1-Trifluoro-5,5-dimethylhexane-2,4-dionate(−)]

M. Ryazanov,[†] V. Nikiforov,[†] F. Lloret,[‡] M. Julve,[‡] N. Kuzmina,[†] and A. Gleizes*[,§]

Moscow State University, Department of Chemistry, Leninskie Gory, 119899 Moscow, Russia, Departament de Química Inorgànica, Facultat de Química de la Universitat de València, Dr. Moliner 50, 46100 Burjassot (València), Spain, CIRIMAT UMR CNRS n°5085, ENSIACET, Institut National Polytechnique de Toulouse, 118 Route de Narbonne, 31077 Toulouse Cedex 4, France

Received October 17, 2001

[Cu(salen)Gd(pta)$_3$] (**1**), [Cu(acacen)Gd(pta)$_3$] (**2**), and [Cu(acacen)Gd(hfa)$_3$] (**3**) are three heterobimetallic [$Cu^{II}Gd^{III}$] complexes of general formula [Cu(SB)Gd(β-dik)$_3$], in which a *N,N′,O,O′* Schiff base (SB) ligand [acacen = *N,N′*-ethylenebis(acetylacetoniminate(−)), salen = *N,N′*-ethylenebis(salicylideneiminate(−))] tetracoordinates Cu^{II} and chelates Gd^{III} as a tris(β-diketonate) complex [hfa = 1,1,1,5,5,5-hexafluoropentane-2,4-dionate(−); pta = 1,1,1-trifluoro-5,5-dimethylhexane-2,4-dionate(−)]. They crystallize as a triclinic structure (space group $P\bar{1}$). The cell parameters are a = 9.8616(10) Å, b = 12.1976(13) Å, c = 18.4187(22) Å, α = 90.671(14)°, β = 100.588(13)°, γ = 103.684(12)°, V = 2113 Å^3, and Z = 2 for **1**; a = 9.7560(11) Å, b = 12.2924(13) Å, c = 18.9368(22) Å, α = 88.449(14)°, β = 87.269(14)°, γ = 67.629(12)°, V = 2098 Å^3, and Z = 2 for **2**; and a = 12.5726(15) Å, b = 15.5985(18) Å, c = 18.3724(21) Å, α = 85.963(13)°, β = 85.411(14)°, γ = 80.766(14)°, V = 3539 Å^3, and Z = 4 for **3**. The Cu(O,O′)Gd bridging cores show folding angles about O,O′ in the range 139°–147° and intramolecular Cu···Gd distances of about 3.3 Å. In the solid state, the molecules form centrosymmetric pseudodimers [Cu(SB)Gd(β-dik)$_3$]$_2$, through the overlap of the Cu(SB) entities. Resulting intradimer Cu···Cu distances are 5.941(1) Å for **1**, 4.831(1) Å for **2**, and 4.511(1) and 3.868(1) Å for **3** which comprises two symmetrically independent dimers. The temperature dependence of complexes **1**–**3** was investigated in the range 1.8–300 K and revealed weak ferromagnetic interactions. Results are discussed in light of the structural features and of available magnetostructural data for other heterobimetallic [$Cu^{II}Gd^{III}$] complexes, including [Cu(salen)Gd(hfa)$_3$] (**4**) (Ramade, I.; Kahn, O.; Jeannin, Y.; Robert, F. *Inorg. Chem.* **1997**, *36*, 930–936).

Introduction

A great number of various investigations have made the magnetic coupling between 3d ions within homo- and heteronuclear metalorganic complexes a well documented topic. The mechanism of interaction can be modeled in a rather satisfactory way, especially when the interacting ions do not possess first-order orbital momentum.[2] The magnetic coupling between 3d and 4f ions is less well understood. Several heterobimetallic complexes associating Cu^{II} and Gd^{III} have been investigated because of the simplifying spin-only character of the magnetic moments of the two ions ($^2S_{1/2}$ and $^8S_{7/2}$). Starting with pioneering works by Gatteschi and

* To whom correspondence should be addressed. E-mail: agleizes@ensct.fr.
[†] Moscow State University.
[‡] Universitat de València.
[§] Institut National Polytechnique de Toulouse.

(1) Ramade, I.; Kahn, O.; Jeannin, Y.; Robert, F. *Inorg. Chem.* **1997**, *36*, 930−936.
(2) Kahn, O. *Molecular Magnetism*; VCH: New York, 1993.

10.1021/ic0110777 CCC: $22.00
Published on Web 03/08/2002

co-workers on a series of [$Cu^{II}Gd^{III}Cu^{II}$] trinuclear species,[3,4] several works on heterodinuclear[1,5−8] and heteropolynuclear complexes[6,9,10−12] containing $Gd^{III}Cu^{II}$ pairs convergently concluded that the $Gd^{III}-Cu^{II}$ intramolecular interaction was ferromagnetic. Very recently, Costes et al. observed antiferromagnetic coupling in Cu−Gd and Cu−Gd−Cu associations through μ-phenolato-μ-oximato bridging.[13,14] The [$Cu^{II}Gd^{III}$] heterobinuclear complexes presenting a ferromagnetic coupling studied so far[1,5−8] have CuO_2Gd bridging cores which mainly differ by their Cu−O−O−Gd dihedral angles. Although the ferromagnetic coupling constant J does not overpass a few reciprocal centimeters, the Cu−O−O−Gd dihedral angle has been shown to dramatically influence the coupling,[1] a rule of thumb being that the highest J values correspond to the more flattened core geometries.

In the course of investigations about volatile heterobimetallic complexes as single source precursors for the chemical vapor deposition of heterobimetallic thin film materials, we have developed the use of preformed neutral 3d metal complexes MX that can act as ligands to coordinatively saturate lanthanide(III) cations in their tris(β-diketonato) complexes, Ln(β-dik)$_3$, thus leading to heterobimetallic complexes of general formula (MX)Ln(β-dik)$_3$.[15−19]

Some of these complexes associate the cations Cu^{II} and Gd^{III}.[16,17] We present here results about syntheses, crystal structures, and magnetic characterizations for a series of novel compounds, [Cu(salen)Gd(pta)$_3$] (**1**), [Cu(acacen)Gd(pta)$_3$] (**2**), and [Cu(acacen)Gd(hfa)$_3$] (**3**), with general formula [Cu(SB)Gd(β-dik)$_3$], where β-dik is either 1,1,1,5,5,5-hexafluoropentane-2,4-dionate (hfa) or 1,1,1-trifluoro-5,5-dimethylhexane-2,4-dionate (pta), and SB is a deprotonated tetradentate Schiff base ligand obtained from the condensation of 1,2-diaminoethane with either salicylic aldehyde (salen) or acetylacetone (acacen). The fourth member of the series, [Cu(salen)Gd(hfa)$_3$] (**4**), has already been described.[1]

Experimental Section

Materials. All chemicals were purchased from standard sources and used as received. Starting compounds H_2acacen, H_2salen, [Cu(acacen)], and [Cu(salen)] were synthesized according to literature methods [20,21] from 1,2-diaminoethane, acetylacetone, salicylic aldehyde, and copper acetate. [Gd(pta)$_3$] and Gd(hfa)$_3$ were obtained by vacuum sublimation (200−220 °C, 0.01 Torr) of the corresponding bis-aqua complexes Gd(β-dik)$_3$(H_2O)$_2$ (dik = pta, hfa), synthesized according to standard procedures.[22,23] Elemental analysis (C, H, N) was performed by the Microanalytical Service of Moscow State University.

Syntheses. All three complexes were synthesized in a similar way. For instance, to prepare [Cu(acacen)Gd(pta)$_3$] (**2**), a 0.5 mmol (143 mg) of Cu(acacen) in chloroform was slowly added to 0.5 mmol (371 mg) of Gd(pta)$_3$ in chloroform. The resulting violet solution was heated under reflux for 1 h. Purple crystals suitable for X-ray analysis deposited on slow evaporation and were filtered off. Yield 90%. [Cu(salen)Gd(pta)$_3$] (**1**) and [Cu(acacen)Gd(hfa)$_3$] (**3**) were prepared in the same way using Gd(hfa)$_3$ and Cu(salen) instead of Gd(pta)$_3$ and Cu(acacen). Anal. Calcd for $C_{40}H_{44}N_2O_8F_9$CuGd (**1**): C, 44.79; H, 4.13; N, 2.61. Found: C, 45.6; H, 4.0; N, 2.5. IR (KBr pellets, cm^{-1}): ν(C−C) 1540; ν(C−O) 1640; ν(C−F) 1260, 1190, 1140. Calcd for $C_{36}H_{48}N_2O_8F_9$CuGd (**2**): C, 30.47; H, 1.99; N, 2.63. Found: C, 30.5; H, 2.1; N, 2.5. IR (KBr pellets, cm^{-1}): ν(C−C) 1550; ν(C−O) 1670; ν(C−F) 1260, 1210, 1150. Calcd for $C_{27}H_{21}N_2O_8F_{18}$CuGd (**3**): C, 42.04; H, 4.70; N, 2.72. Found: C, 42.2; H, 4.6; N, 2.6. IR (KBr pellets, cm^{-1}): ν(C−C) 1535; ν(C−O) 1635; ν(C−F) 1255, 1185, 1145.

Physical Measurements. IR spectra were recorded on a Perkin-Elmer 1750 FTIR spectrophotometer with KBr disks in the 4000−400 cm^{-1} region. Magnetic susceptibility measurements (1.9−290 K) for polycrystalline samples of complexes **1**−**3** were performed with a Quantum Design superconducting quantum interference device (SQUID) magnetometer using applied magnetic fields of 1 T (high-temperature range) and 100 G (low-temperature range). The magnetometer was calibrated with $(NH_4)_2Mn(SO_4)_2\cdot 12H_2O$. The experimental susceptibility data were corrected for the diamagnetism of the constituent atoms.

X-ray Structure Determinations. The crystals were mounted on a Stoe imaging plate diffraction system (IPDS), equipped with an Oxford Cryosystems cooler device. The data were collected at 120 K, with graphite-monochromatized Mo Kα radiation (λ = 0.71073 Å), using φ rotation (**1**) or oscillation (**2**, **3**) movement mode. Crystal sizes were 0.22 × 0.17 × 0.10 mm^3 (**1**), 0.25 × 0.20 × 0.16 mm^3 (**2**), and 0.40 × 0.33 × 0.23 mm^3 (**3**). Crystal decays were monitored by measuring 200 reflections per image; only statistical fluctuations were observed. Intensities were corrected for Lorentz and polarization effects, not for absorption (average cylindrical μr = 0.2 (**1**), 0.2 (**2**), 0.5 (**3**)). The structures were solved

(3) Bencini, A.; Benelli, C.; Caneschi, A.; Carlin, R. L.; Dei, A.; Gatteschi, D. *J. Am. Chem. Soc.* **1985**, *107*, 8128−8136.
(4) Bencini, A.; Benelli, C.; Caneschi, A.; Dei, A.; Gatteschi, D. *Inorg. Chem.* **1986**, *25*, 572−575.
(5) Costes, J.-P.; Dahan, F.; Dupuis, A. *Inorg. Chem.* **2000**, *39*, 165−168.
(6) Costes, J.-P.; Dahan, F.; Dupuis, A.; Laurent, J.-P. *New J. Chem.* **1998**, 1525−1529.
(7) Costes, J.-P.; Dahan, F.; Dupuis, A.; Laurent, J.-P. *Inorg. Chem.* **1997**, *36*, 3429−3433.
(8) Costes, J.-P.; Dahan, F.; Dupuis, A.; Laurent, J.-P. *Inorg. Chem.* **1996**, *35*, 2400−2402.
(9) Sanz, J. L.; Ruiz, R.; Gleizes, A.; Lloret, F.; Faus, J.; Julve, M.; Borras-Almenar, J. J.; Journaux, Y. *Inorg. Chem.* **1996**, *35*, 7384−7393.
(10) Benelli, C.; Blake, A. J.; Milne, P. E. Y.; Rawson, J. M.; Winpenny, R. E. P. *Chem.—Eur. J.* **1995**, *1*, 614−618.
(11) Andruh, M.; Ramade, I.; Codjovi, E.; Guillou, O.; Kahn, O.; Trombe, J.-C. *J. Am. Chem. Soc.* **1993**, *115*, 1822−1829.
(12) Guillou, O.; Oushoorn, R. L.; Kahn, O.; Boubekeur, K.; Batail, P. *Angew. Chem., Int. Ed. Engl.* **1992**, *31*, 626−628.
(13) Costes, J.-P.; Dahan, F.; Dupuis, A.; Laurent, J.-P. *Inorg. Chem.* **2000**, *39*, 169−173.
(14) Costes, J.-P.; Dahan, F.; Dupuis, A. *Inorg. Chem.* **2000**, *39*, 5994−6000.
(15) Gleizes, A.; Julve, M.; Kuzmina, N.; Alikhanyan, A.; Lloret, F.; Malkerova, I.; Sanz, J. L.; Senocq, F. *Eur. J. Inorg. Chem.* **1998**, 1169−1174.
(16) Gleizes, A. N.; Senocq, F.; Julve, M.; Sanz, J. L.; Kuzmina, N.; Troyanov, S.; Malkerova, I.; Alikhanyan, A.; Ryazanov, M.; Rogachev, A.; Dedlovskaya, E. *J. Phys. IV* **1999**, *9*, 943−951.
(17) Kuzmina, N. P.; Rogachev, A. Y.; Spiridinov, F. M.; Dedlovskaya, E. M.; Ketsko, V. A.; Gleizes, A.; Battiston, G. *Russ. J. Inorg. Chem.* **1999**, *45*, 1340−1347.
(18) Kuzmina, N.; Ryazanov, M.; Malkerova, I.; Alikhanyan, A.; Gleizes, A. N. *Eur. J. Inorg. Chem.* **2001**, 701−706.
(19) Alikhanyan, A. S.; Malkerova, I. P.; Kuz'mina, N. P.; Gleizes, A.; Julve-Olcina, M.; Sanz, J. L.; Eremenko, I. L. *Russ. J. Inorg. Chem.* **1999**, *44*, 907−910.
(20) McCarthy, P. J.; Hovey, R. J.; Keihei, U.; Martell, A. E. *J. Am. Chem. Soc.* **1955**, *77*, 5820−5824.
(21) Kirson, B.; Ucma, S. *Bull. Soc. Chim. Fr.* **1966**, 2236−2240.
(22) Shigematsu, S.; Matsui, M.; Utsunomia, K. *Jpn. Bull. Chem. Soc.* **1969**, *42*, 1278−1281.
(23) Richardson, M. F.; Wagner, D. F.; Sands, D. E. *J. Inorg. Nucl. Chem.* **1968**, *30*, 1275−1279.

Table 1. Crystal Data for Compounds **1**−**3**

	[Cu(salen)Gd(pta)$_3$] (**1**)	[Cu(acacen)Gd(pta)$_3$] (**2**)	[Cu(acacen)Gd(hfa)$_3$] (**3**)
chemical formula	$GdCuC_{40}H_{44}F_9N_2O_8$	$GdCuC_{36}H_{48}F_9N_2O_8$	$GdCuC_{27}H_{21}F_{18}N_2O_8$
fw	1072.56	1028.55	1064.25
space group	$P\bar{1}$ (No. 2)	$P\bar{1}$ (No. 2)	$P\bar{1}$ (No. 2)
a (Å)	9.8616(10)	9.7560(11)	12.5726(15)
b (Å)	12.1976(13)	12.2924(13)	15.5985(18)
c (Å)	18.4187(22)	18.9368(22)	18.3724(21)
α (deg)	90.671(14)	88.449(14)	85.963(13)
β (deg)	100.588(13)	87.269(14)	85.411(14)
γ (deg)	103.684(12)	67.629(12)	80.766(14)
V, (Å^3)	2112.5(4)	2097.6(4)	3538.9(7)
Z	2	2	4
D_{calcd} (g cm^{-1})	1.686	1.628	1.997
T (°C)	−153	−153	−153
radiation (λ(Å))	Mo Kα (0.71073)	Mo Kα (0.71073)	Mo Kα (0.71073)
μ (cm^{-1})	21.5	21.6	26.0
R^a	0.022	0.039	0.040
$R_w{}^b$	0.055	0.092	0.112

[a] $R = \sum||F_o| - |F_c||/\sum|F_o|$. [b] $R_w = \{\sum[w(F_o^2 - F_c^2)^2/\sum[w(F_o^2)^2\}^{1/2}$.

by the Patterson method[24] and refined by full-matrix least-squares.[25] All H atoms were introduced at calculated positions using a riding model. Non-H atoms were attributed anisotropic displacement parameters. Refinements were on F_o^2 for all reflections. Weighted reliability factors R_w and goodness of fit factors S were based on F_o^2. Conventional R factors were based on F_o ($F_o > 4\sigma(F_o)$). The crystallographic data are summarized in Table 1.

Description and Comparison of the Structures

Hereafter, [Cu(salen)Gd(pta)$_3$], [Cu(acacen)Gd(pta)$_3$], and [Cu(acacen)Gd(hfa)$_3$] are referred to as CuSGdP (**1**), CuAGdP (**2**), and CuAGdH (**3**), respectively. One goes from one compound to the next one by substituting acacen to salen about copper (**1** → **2**) and then hfa to pta about Gd (**2** → **3**).

Common Features to the Three Structures. The three crystal structures comprise [Cu(SB)Gd(β-dik)$_3$] heterodimetallic complex molecules in which oxygen atoms O(1) and O(2) from the neutral copper Schiff base complex Cu(SB) chelates the gadolinium(III) tris(β-diketonato(−)) complex, Gd(β-dik)$_3$. In CuAGdH, there are two symmetrically independent molecules, hereafter referred to as CuAGdH-1 and CuAGdH-2. Views of the molecules with atoms numbering schemes are given in Figure 1 for CuSGdP, Figure 2 for CuAGdP, and Figure 3 for CuAGdH. Selected distances and angles are synoptically displayed in Table 2.

The copper atoms have nearly square planar coordination geometries (vide infra). The gadolinium atoms have 8-fold coordination geometries intermediary between pseudosquare antiprismatic and bicapped trigonal prismatic. For CuSGdP, the square faces are delimited by atoms O(1), O(1a), O(2a), O(2c) and O(2), O(1b), O(2b), O(1c) with intraplane O···O distances ranging from 2.725 to 3.344 Å and from 2.727 to 2.886 Å, respectively. The dihedral angle between upper and lower planes is 3.9°. For CuAGdP, the square faces are delimited by atoms O(1), O(2a), O(1c), O(2c) and O(2), O(1a), O(1b), O(2b) with intraplane O···O distances ranging from 2.684 to 3.425 Å and from 2.779 to 2.873 Å, respectively. The dihedral angle between upper and lower planes is 5.6°. For CuAGdH-1, the square faces are delimited

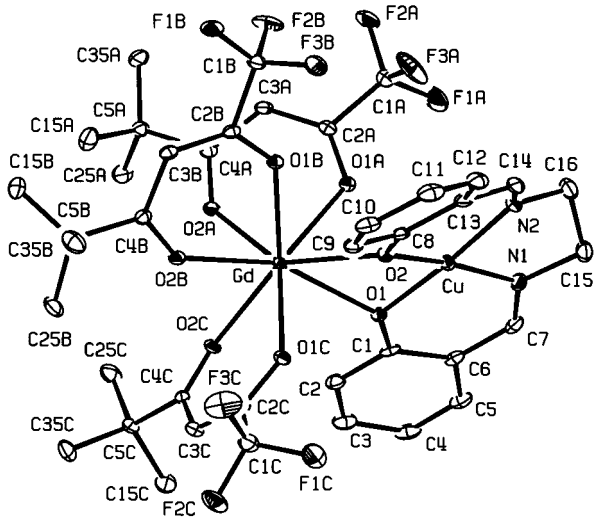

Figure 1. ORTEP plot for [Cu(salen)Gd(pta)$_3$] (**1**) (30% probability level ellipsoids).

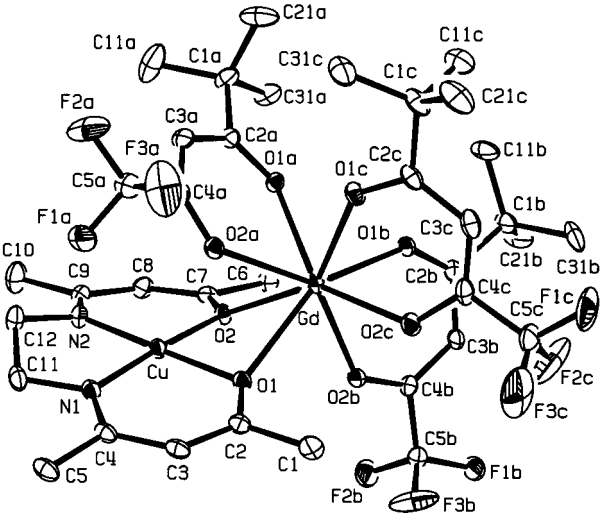

Figure 2. ORTEP plot for [Cu(acacen)Gd(pta)$_3$] (**2**) (30% probability level ellipsoids).

(24) Sheldrick, G. M. *SHELXS-97: Program for Crystal Structure Solution*; University of Göttingen: Göttingen, Germany, 1990.
(25) Sheldrick, G. M. *SHELXL-97: Program for the Refinement of Crystal Structures from Diffraction Data*; University of Göttingen: Göttingen, Germany, 1997.

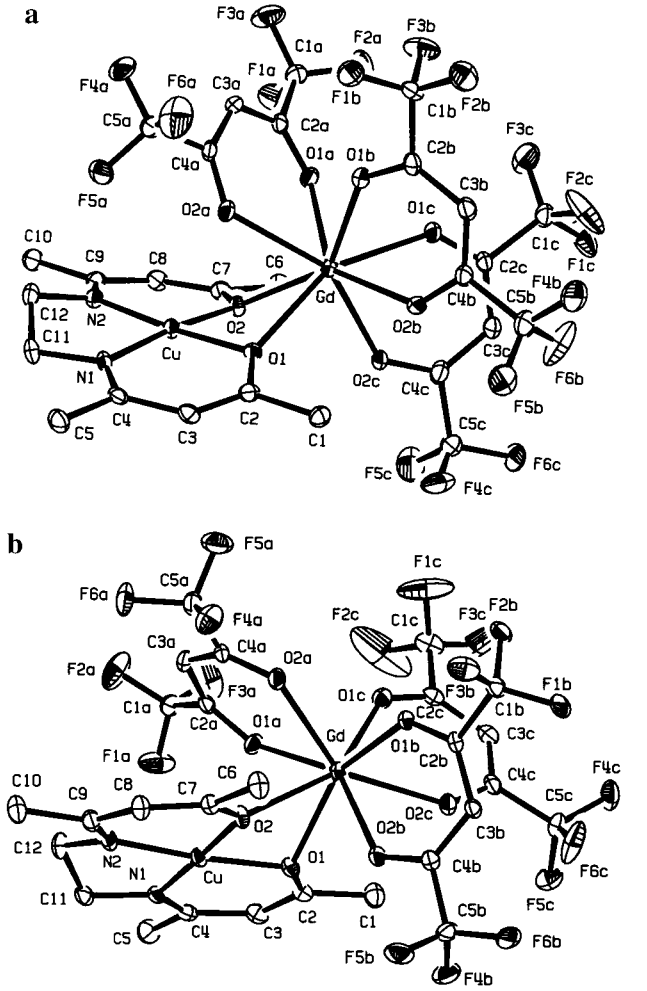

Figure 3. ORTEP plots for the two symmetrically independent molecules in [Cu(acacen)Gd(hfa)$_3$] (**3**), (a) CuAGdH-1 and (b) CuAGdH-2 (30% probability level ellipsoids).

by atoms O(1), O(1b), O(2a), O(2b) and O(2), O(1a), O(1c), O(2c), with intraplane O···O distances ranging from 2.726 to 3.302 Å and from 2.685 to 2.995 Å, respectively. The angle between upper and lower plane is 3.7°. For CuAGdH-2, the square faces are delimited by atoms O(1), O(1a), O(1c), O(2c) and O(2), O(2a), O(1b), O(2b), with intraplane O···O distances ranging from 2.799 to 2.895 Å and from 2.703 to 3.438 Å, respectively. The dihedral angle between the upper and lower planes is 9.3°.

Dihedral angles CuO(1)O(2)Gd about segments O(1)O(2) are in the range 139°−147°. Deviations from planarity in the Cu(SB) entities result from the ethanediamino N−C−C−N diedral angles ranging from 31° to 42°. The [Cu(SB)Gd(β-dik)$_3$] molecules pair into pseudodimers through inversion symmetry and overlapping of Cu(SB) moieties. The different ligands lead to fine structural differences in molecular geometries and in molecular interactions as well.

Crystal Structures. CuSGdP and CuAGdP have triclinic unit cells, with similar volumes of 2112 and 2098 Å^3, respectively. The unit cell comprises two heterodinuclear units, Cu($C_{15}H_{14}O_2N_2$)Gd($C_8H_{10}O_2F_3$)$_3$ for CuSGdP and Cu($C_{12}H_{18}O_2N_2$)Gd($C_8H_{10}O_2F_3$)$_3$ for CuAGdP. In the two structures, these units pair into pseudodimers (CuSGdP)$_2$ or (CuAGdP)$_2$ through inversion and overlapping of Cu($C_{15}H_{14}O_2N_2$) (Figure 4a) or Cu($C_{12}H_{18}O_2N_2$) moieties (Figure 5a). The intermolecular copper−copper separation is more than 1 Å larger for CuSGdP (5.94 Å) than for CuAGdP (4.83 Å).

For CuAGdH, the unit cell is still triclinic. It has a volume of 3539 Å^3. It comprises two symmetrically independent sets of two heterodinuclear units Cu($C_{12}H_{18}O_2N_2$)Gd($C_5HO_2F_6$)$_3$ referred to as CuAGdH-1 and CuAGdH-2. The same pairing effect as in CuSGdP takes place through centrosymmetric overlap of the Cu($C_{12}H_{18}O_2N_2$) moieties, resulting in two symmetrically independent pseudodimers per unit cell, (CuAGdH-1)$_2$ (Figure 5b) and (CuAGdH-2)$_2$ (Figure 5c). The intermolecular copper−copper separations are significantly different: 4.51 Å in (CuAGdH-1)$_2$ and 3.87 Å in (CuAGdH-2)$_2$. Moreover, they are shorter than in CuSGdP (5.94 Å) and in CuAGdP (4.83 Å). The different intradimer Cu···Cu separations are roughly related to different N−C−C−N dihedral angles for the Schiff base ligands. The torsion is much more pronounced for salen (42°) in CuSGdP than for acacen (35° and 33° in CuAGdH; 31° in CuAGdP). In the acacen derivatives, overlapping parts are delimited by atoms Cu, O(1), N(1), N(2), C(1) to C(5), C(11), C(12). Atom-to-mean plane deviations for these fragments are reported in Table 2, along with root-mean-square deviations of fitted atoms and distances between centrosymmetrically related overlapping mean planes. The shortest Cu···Cu distance in CuAGdH-2 with respect to CuAGdH-1 is consistent with observed values for respective rms deviations of atoms and distances between mean planes. According to these parameters, the Cu···Cu distance for CuAGdP should be as short as or even shorter than that for CuAGdH-2. The difference most likely results from steric hindrances and/or packing effects which might hinder the overlap in CuAGdP and CuAGdH-1 with respect to CuAGdH-2. Because of *tert*-butyl substituting to trifluoromethane groups, CuAGdP has more encumbered β-diketonate ligands than CuAGdH. Therefore, the differences between CuAGdP and CuAGdH may originate in steric hindrance. The fact that CuAGdP and CuAGdH-1 have resembling overlap schemes which neatly differ from that of CuAGdH-2 might be related to different spatial distributions of the β-diketonate ligands about Gd in the three molecules. In CuAGdP (Figure 5a) and CuAGdH-1 (Figure 5b), the β-diketonate O atoms show similar orientations about Gd with respect to the Cu(SB) entity. For CuAGdH-2 (Figure 5c), these orientations are different. The configuration of the β-diketonate ligands about Gd might well generate less hindering interactions between the overlaping parts in CuAGdH-2 that in CuAGdP and CuAGdH-1.

The case of the salen derivative is discussed in next paragraph.

Comparison between the Structures of [Cu(salen)Gd(hfa)$_3$][1] and [Cu(salen)Gd(pta)$_3$]. It is interesting to compare the structures of these two compounds which only differ by replacing one of the two CF_3 groups by a $C(CH_3)_3$ group in the β-diketonate ligands. For [Cu(salen)Gd(hfa)$_3$], the dimeric association of the molecules is pseudocentrosymmetric, and the Cu···Cu separation is as low as 3.630(3) Å[1] to compare

Table 2. Selected Distances (Å) and Angles (deg) for Compounds **1**−**3**

	[Cu(salen)Gd(pta)$_3$] CuSGdP (**1**)	[Cu(acacen)Gd(pta)$_3$] CuAGdP (**2**)	[Cu(acacen)Gd(hfa)$_3$] CuAGdH-1 (**3**)	[Cu(acacen)Gd(hfa)$_3$] CuAGdH-2 (**3**)
Gd−O(1)	2.495(2)	2.478(2)	2.427(3)	2.457(3)
Gd−O(2)	2.369(2)	2.394(2)	2.408(3)	2.391(3)
Gd−O(1a)	2.412(2)	2.392(2)	2.351(3)	2.401(3)
Gd−O(2a)	2.340(2)	2.366(2)	2.404(3)	2.375(4)
Gd−O(1b)	2.339(2)	2.337(2)	2.355(4)	2.342(3)
Gd−O(2b)	2.360(2)	2.375(3)	2.342(3)	2.388(3)
Gd−O(1c)	2.368(2)	2.367(3)	2.360(3)	2.366(3)
Gd−O(2c)	2.371(2)	2.327(3)	2.369(3)	2.366(3)
Cu−O(1)	1.930(2)	1.950(2)	1.957(3)	1.954(3)
Cu−O(2)	1.912(2)	1.924(2)	1.926(3)	1.924(3)
Cu−N(1)	1.922(2)	1.910(3)	1.920(4)	1.914(4)
Cu−N(2)	1.929(2)	1.924(3)	1.925(4)	1.929(4)
O(1)−Cu−O(2)	87.46(7)	84.5(1)	83.9(1)	84.6(1)
O(1)−Cu−N(1)	95.85(9)	95.8(1)	95.4(1)	95.9(2)
O(1)−Cu−N(2)	174.83(9)	177.4(1)	175.3(2)	175.3(2)
O(2)−Cu−N(1)	169.13(9)	175.1(1)	173.5(2)	178.6(2)
O(2)−Cu−N(2)	93.31(9)	93.0(1)	94.8(1)	93.2(2)
N(1)−Cu−N(2)	84.32(10)	86.5(1)	86.3(2)	86.1(2)
Cu···Gd	3.2883(5)	3.2737(8)	3.2883(7)	3.3130(7)
Cu···Cu	5.941(1)	4.831(1)	4.511(1)	3.868(1)
		Dihedral Angles		
Cu−O(1)−O(2)−Gd	146.91(8)	138.6(1)	141.0(1)	144.2(1)
N(1)−C(i)−C(i + 1)−N(2)	42.2(3)	31.0(5)	34.7(6)	32.7(6)
		Mean Plane		
O(1)*[a]	0.128(1)	0.031(2)	−0.092(2)	0.025(2)
O(2)*	−0.131(1)	−0.032(2)	0.093(2)	−0.025(2)
N(1)*	−0.131(1)	−0.031(2)	0.091(2)	−0.025(2)
N(2)*	0.134(1)	0.032(2)	−0.092(2)	0.025(2)
Cu	0.044(1)	0.050(2)	−0.016(2)	−0.046(2)
		Mean Plane		
Cu*		0.005(2)	0.026(2)	−0.029(2)
O(1)*		0.036(3)	−0.159(3)	0.012(3)
N(1)*		0.093(3)	−0.024(4)	−0.106(4)
N(2)*		−0.069(2)	0.062(2)	0.074(3)
C(1)*		−0.051(3)	0.078(4)	0.044(4)
C(2)*		0.015(3)	−0.009(5)	−0.001(5)
C(3)*		−0.004(4)	0.069(5)	−0.044(5)
C(4)*		0.026(3)	−0.010(5)	−0.038(5)
C(5)*		−0.051(2)	−0.034(4)	0.089(4)
rms deviations of fitted atoms		0.048	0.069	0.059
distance between overlapping mean planes		3.478(4)	3.671(4)	3.492(5)

[a] Asterisk indicates atoms included in mean plane calculations.

with that of 5.941(1) Å for [Cu(salen)Gd(pta)$_3$]. The distance of 3.63 Å is practically what can be expected from two planar systems with van der Waals interactions between π-electrons. Even if the authors did not describe precisely the overlap scheme for [Cu(salen)Gd(hfa)$_3$], it is most likely similar to the one in the isostructural Ni derivative, [Ni(salen)Gd(hfa)$_3$] (Ni···Ni = 3.583(3) Å).[15] The overlap scheme for [Ni(salen)-Gd(hfa)$_3$] is shown in Figure 4b. Each Ni atom lies in front of a six-membered NiONC$_3$ ring of the opposite molecule, so as to give a very short Ni···Ni distance. The driving interaction is most likely to occur between π-electrons from a phenyl ring of one molecule and π-electrons from the NiONC$_3$ ring of the other molecule. In [Cu(salen)Gd(pta)$_3$], each Cu cation lies almost above the most external phenyl C−C bond of a phenyl ring of the opposite molecule. This bond, namely C(4)−C(5), is the shortest one in the phenyl ring, measuring 1.363(5) Å while the other bonds range from 1.382(4) to 1.419(4) Å. The same bond length distribution occurs in the other phenyl ring which has no facing salen part. An intermolecular interaction involving π-electrons from the rather electron rich C(4)−C(5) bond and copper d_{z^2} electrons is likely to occur as shown by Cu···C(4) and Cu···C(5) distances as short as 3.332(3) and 3.191(3) Å, respectively. The bond Cu−N(1) lies above the phenyl ring, leading to N(1)···C(1) and N(1)···C(2) separations of 3.60 and 3.58 Å, respectively. Cu is at 3.164(2) Å and N(1) at 3.423(3) Å from the mean plane of the facing phenyl ring (Figure 4a).

Comparative Description of the N_2CuO_2Gd Cores. Since the compounds have been submitted to magnetism investigations, it is interesting to comparatively describe the N_2CuO_2Gd cores in the three molecules. The three compounds have Cu−O bond lengths significantly differing from each other by about 0.02 Å in CuSGdP and 0.03 Å in CuAGdP and in either molecule of CuAGdH (Table 2). Moreover, they are longer in the latter compounds (ligand

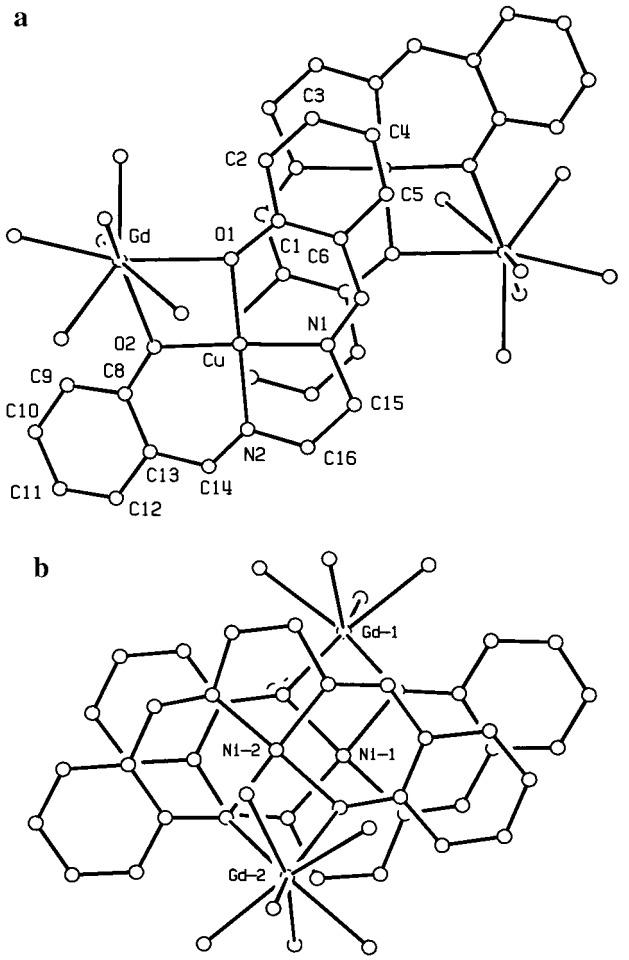

Figure 4. Overlap schemes for (a) two centrosymmetrically related Cu(salen)GdO_6 entities in [Cu(salen)Gd(pta)$_3$] (**1**) and (b) two noncentrosymmetrically related Ni(salen)GdO_6 entities in [Ni(salen)Gd(hfa)$_3$] which is isostructural with [Cu(salen)Gd(hfa)$_3$] (**4**) (see text).

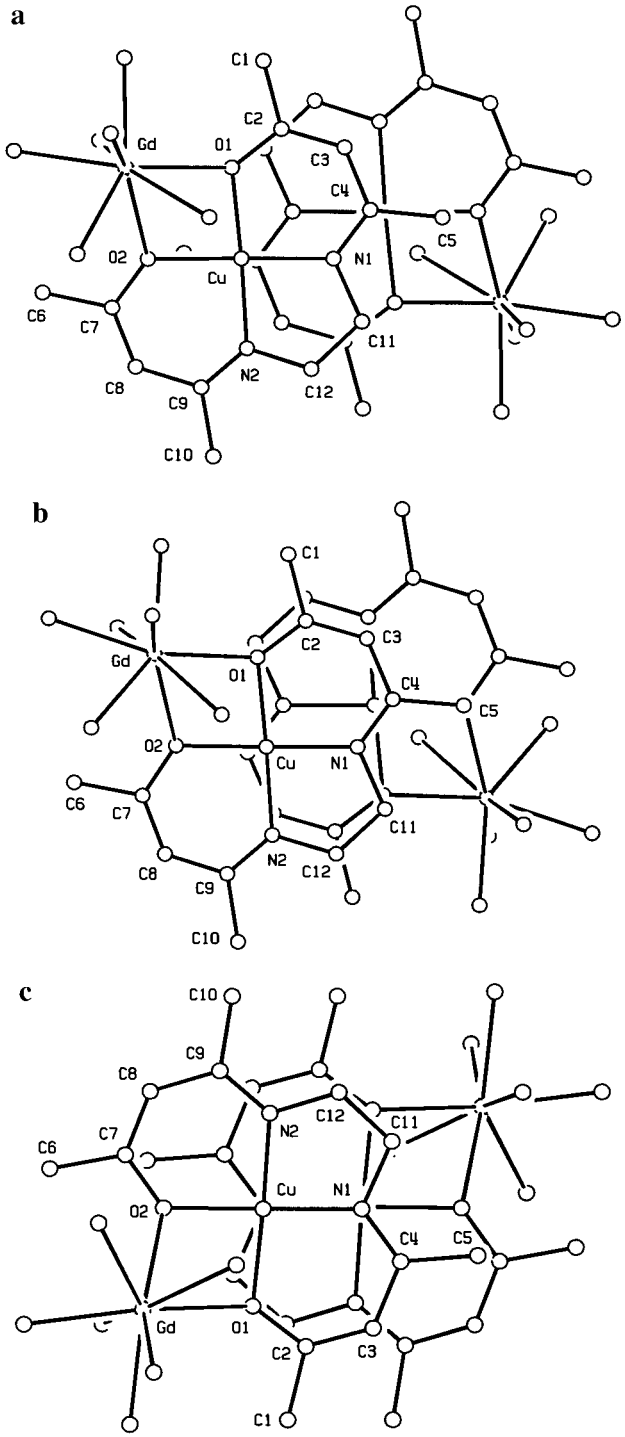

Figure 5. Overlap schemes for two centrosymmetrically related Cu(acacen)GdO_6 entities in (a) compound **2**, (b) compound **3**, molecule CuAGdH-1, and (c) compound **3**, molecule CuAGdH-2.

acacen) than in the former (ligand salen). The Cu−N bond lengths do not significantly differ within every molecule as well as from one molecule to the other one.

Deviations from planarity within CuO_2N_2 chromophores differ from one molecule to the other. Atom-to-mean plane distances for atoms O(1), O(2), N(1), and N(2) show significant, slight tetrahedral deformations for the three molecules, with distances equal to 0.13 Å for CuSGdP and 0.09 Å for CuAGdH-1, but only 0.03 Å for CuAGdP and CuAGdH-2. Whereas Cu stands within the "flattened tetrahedron" in CuSGdP and CuAGdH-1, it stands out of it in CuAGdP and CuAGdH-2, as shown by copper distances to mean planes of atoms O(1), O(2), N(1), and N(2) in Table 2.

Another interesting structural feature to examine in view of magnetic properties is the geometry of the CuOOGd bridge. Averaged Gd−O(1) and Gd−O(2) distances in the three molecules are almost equal: 2.432 Å for CuSGd, 2.436 Å for CuAGdP, and 2.418 and 2.424 Å for CuAGdH. The two bond lengths markedly differ by 0.13 Å in CuSGdP, 0.08 Å in CuAGdP, and 0.07 Å in CuAGdH-2. The difference is less marked in CuAGdH-1 (0.02 Å). Folding angles about O(1)O(2) range from 139° to 147°. The Cu···Gd distances do not much differ from one molecule to the other: 3.288 Å in CuSGdP, 3.274 Å in CuAGdP, 3.288 Å in CuAGdH-1, and 3.313 Å in CuAGdH-2.

Magnetic Properties of Complexes 1−3

The magnetic properties of complexes **1**−**3** under the form of the $\chi_M T$ products versus T (χ_M is the magnetic susceptibility for a $Gd^{III}Cu^{II}$ pair) are shown in Figure 6. At room temperature, the value of $\chi_M T$ for **1**−**3** is ∼8.32 $cm^3 \cdot mol^{-1} \cdot K$, which corresponds to what is expected for magnetically

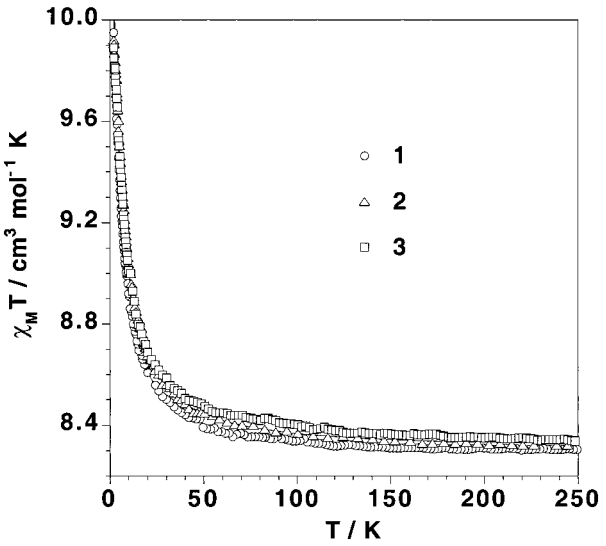

Figure 6. Thermal variations of $\chi_M T$ for complexes **1**−**3**: experimental data (○,△,□) and best-fit curves (−).

isolated Gd^{III} and Cu^{II} ions. Upon cooling, the values remain constant until 150 K and continuously increase at lower temperatures, reaching values of 9.95 (**1**), 9.92 (**3**), and 9.89 (**2**) $cm^3 \cdot mol^{-1} \cdot K$ at 1.9 K. The shapes of $\chi_M T$ versus T plots for **1**−**3** indicate ferromagnetic $Gd^{III}-Cu^{II}$ interactions, with $S = 4$ low-lying states and $S = 3$ excited states. The fact that the nonet ground spin state is not fully populated at 1.9 K accounts for the lack of the predicted plateau for $\chi_M T$ at very low temperatures. Analyses of the magnetic data for **1**−**3** have been carried out through the Hamiltonian $H = -JS_{Gd} \cdot S_{Cu}$, where J is the exchange coupling parameter and S_{Gd} and S_{Cu} are the spin operators associated to the interacting spin centers. The theoretical expression for $\chi_M T$ is given by eq 1

$$\chi_M T = \frac{4N\beta^2}{k} \frac{7g_3^2 + 15g_4^2 \exp(4J/kT)}{7 + 9\exp(4J/kT)} \quad (1)$$

where g_3 and g_4 are the Zeeman factors associated with the $S = 3$ and $S = 4$ low-lying states, respectively. In addition, g_3 and g_4 are dependent on the local Zeeman factors through eqs 2 and 3.[2]

$$g_3 = (9g_{Gd} - g_{Cu})/8 \quad (2)$$

$$g_4 = (7g_{Gd} + g_{Cu})/8 \quad (3)$$

Least-squares fitting of the experimental data through eqs 1−3 leads to the following set of parameters: $J = +1.21$ cm^{-1}, $g_{Gd} = 2.00$, $g_{Cu} = 2.10$, and $R = 1.4 \times 10^{-5}$ for **1**; $J = +1.47$ cm^{-1}, $g_{Gd} = 2.00$, $g_{Cu} = 2.05$, and $R = 1.5 \times 10^{-5}$ for **2**; and $J = +1.25$ cm^{-1}, $g_{Gd} = 2.00$, $g_{Cu} = 2.08$, and $R = 1.7 \times 10^{-5}$ for **3**. R is the agreement factor defined as $\Sigma[(\chi_M T)^{calcd} - (\chi_M T)^{obs}]^2/\Sigma[(\chi_M T)^{obs}]$, and its magnitude in the three fits indicates a very good matching between observed and calculated $\chi_M T$ values. The field dependence of the magnetization of **1**−**3** up to 5 T at 1.9 K confirms the ferromagnetic nature of the interaction: the experimental magnetization is clearly above that calculated for the sum of the Brillouin functions of magnetically isolated Gd^{III} and Cu^{II} and slightly below the Brillouin function for an $S = 4$ pair state. The saturation magnetization is close to $8N\beta$.

Scheme 1

$$\underset{\text{Gd(1)-------Cu(1)}\ldots\ldots\text{Cu(2)-------Gd(2)}}{\overset{J_{GdCu}}{\qquad\qquad\qquad\qquad}}$$
$$j_{CuCu}$$

Whereas $[CuSGdP]_2$ in **1**, $[CuAGdP]_2$ in **2**, and $[CuAGdH\text{-}1]_2$ in **3** may be considered as consisting of well isolated $Gd^{III}-Cu^{II}$ heterodinuclear units from the intradimer Cu···Cu distances in the range 4.51−5.94 Å, the rather short Cu···Cu separation of 3.868(1) Å for the other dimer in **3**, $[CuAGdH\text{-}2]_2$, suggests to treat it as a dimer of pairs with intramolecular J_{GdCu} and intermolecular j_{CuCu} interaction parameters (see Scheme 1).

The fitting of the experimental magnetic data for **3** with such a model did neither improve the previous fit nor change significantly the found parameters, the computed j_{CuCu} being practically zero. A similar situation occurs for the complex $[Cu(salen)Gd(hfa)_3]$ (**4**),[1] for which a j_{CuCu} much less than 0.2 cm^{-1} was computed for a significantly shorter intermolecular Cu···Cu separation (3.63 Å in **4** versus 3.87 and 4.51 Å in **3**).

Ferromagnetic interactions observed in **1**−**3** are in agreement with the magnetic studies carried out on structurally characterized heterodinuclear $Gd^{III}-Cu^{II}$ complexes exhibiting the same GdO_2Cu bridging pathway, as can be seen in Table 3. As previously noted,[1,6] the ferromagnetic interaction between Cu^{II} and Gd^{III} increases as fast as the bending at the CuO_2Gd core decreases. Although it has been proposed to correlate the absolute value of J with this dihedral angle,[5] the values listed in Table 3 are too limited, and further experimental work is needed to establish such a correlation. It should be interesting to see if the coupling becomes antiferromagnetic for larger bending values in this series.

Anyway, the ferromagnetic character of the magnetic interaction within the $Cu^{II}O_2Gd^{III}$ core was attributed to the coupling between the 4f−5d ground configuration and the excited configuration coming from the $3d_{Cu} \rightarrow 5d_{Gd}$ electron transfer,[1,11] following a mechanism first suggested by Goodenough.[26] This electron transfer integral involves the singly occupied copper orbital and the five 5d gadolinium orbitals. Given that their largest values would be associated with the gadolinium 5d orbitals oriented along the two Gd−O(bridging atom) directions, one concludes easily that the larger the bending at the O(1)···O(2) hinge the smaller the absolute value of these integrals, and consequently, the weaker the ferromagnetic coupling. Other magnetostructural studies concerning the $Cu^{II}-Gd^{III}$ spin carriers separated by more than 5.5 Å by polyatomic bridges have shown the occurrence of a significant ferromagnetic interaction between these cations in trinuclear,[27] pentanuclear,[9] ladderlike,[28] and tube-

(26) Goodenough, J. B. *Magnetism and the Chemical Bond*; Interscience: New York, 1963.
(27) Benelli, C.; Fabretti, A. C.; Giusti, A. *J. Chem. Soc., Dalton Trans.* **1993**, 409−412.
(28) Guillou, O.; Bergerat, P.; Kahn, O.; Bakalbassis, E.; Boubekeur, K.; Batail, P.; Guillot, M. *Inorg. Chem.* **1992**, *31*, 110−114.

Table 3. Selected Magnetostructural Data for Various Dinuclear $Gd^{III}-Cu^{II}$ Complexes with a GdO_2Cu Bridging Core

compound[a]	Cu−O(1)	Cu−O(2)	O(1)−Cu−O(2)[b]	Gd−O(1)	Gd−O(2)	O(1)−Gd−O(2)[c]	δ[d] (deg)	Gd···Cu[e]	*J*[f]	ref
$[L^1CuCl_2Gd(H_2O)_4]Cl\cdot 2H_2O$	1.981(2)	1.967(3)	78.2(1)	2.335(2)	2.344(2)	64.31(9)	1.7(2)	3.5121(5)	10.1	5
$L^2Cu(OCMe_2)Gd(NO_3)_3$	1.879(5)	1.904(5)	81.8(2)	2.398(5)	2.337(5)	63.0(2)	12.9(2)	3.4275(9)	7.2	8
$L^3{}_2Cu(HOMe)Gd(NO_3)_3$	1.943(2)	1.940(2)	79.31(8)	2.327(2)	2.395(2)	63.29(7)	12.5(2)	3.4842(3)	6.8	7
$L^1Cu(OCMe_2)Gd(NO_3)_3$	1.953(2)	1.952(2)	78.29(9)	2.387(2)	2.390(2)	62.14(7)	16.6(2)	3.5231(4)	4.8	7
$L^1Cu(O_2COMe)Gd(thd)_2$	1.973(3)	1.965(3)	83.04(10)	2.420(3)	2.434(2)	65.07(8)	19.1(2)	3.4727(4)	4.2	6
[(MeIm)(salen)CuGd(hfa)$_3$]	1.91(2)	2.01(2)		2.38(2)	2.39(2)		39.6	3.252(4)	1.42	1
[Cu(salen)Gd(hfa)$_3$]	1.89(1)	1.924(9)	O1O2 2.544	2.48(1)	2.41(1)	O1O2 2.544	47.0	3.198(2)	0.4	1
(2 symmetrically independent molecules)	1.90(1)	1.90(1)	O1O2 2.545	2.45(1)	2.46(1)	O1O2 2.545	49.6	3.231(2)		
[Cu(salen)Gd(pta)$_3$] (**1**)	1.930(2)	1.912(2)	87.46(7)	2.495(2)	2.369(2)	66.13(6)	33.1(1)	3.2883(5)	1.21	*g*
[Cu(acacen)Gd(pta)$_3$] (**2**)	1.950(2)	1.924(2)	84.5(1)	2.478(2)	2.394(2)	64.62(9)	41.4(1)	3.2737(8)	1.47	*g*
[Cu(acacen)Gd(hfa)$_3$] (**3**)	1.957(3)	1.926(3)	83.9(1)	2.427(3)	2.408(3)	65.0(1)	39.0(1)	3.2883(7)	1.25	*g*
(2 symmetrically independent molecules)	1.954(3)	1.924(3)	84.6(1)	2.457(3)	2.391(3)	65.1(1)	35.8(1)	3.3130(7)		

[a] Abbreviations for the names of the ligands: L^1 = 1,3-bis(3-methoxysalicylidene)amino-2,2′-dimethylpropane; L^2 = 1,2-bis(3-methoxysalicylidene)amino-2,2′-dimethylethane; L^3 = 3-methoxysalicylaldiminato; O_2COMe = monomethyl carbonate; Hthd = tetramethylheptanedione; MeIm = 1-methylimidazole; H_2salen = *N*,*N*′-ethylenebis(salicylideneamine); Hhfa = hexafluoroacetylacetone; Hpta = 1,1,1-trifluoro-5,5-dimethylhexane-2,4-dione; H_2acacen = *N*,*N*′-ethylenebis(acetylacetoneimine). [b,c] Values in deg of bond angles at the metal atoms [d] Value in deg of the dihedral angle within the bridging network CuO(1)O(2)Gd taking the O(1)O(2) as the inge. [e] Intramolecular Cu−Gd separation in Å. [f] Value of the magnetic coulping in cm^{-1}. [g] This work.

like[12,29] structures. However, the hypothesis that ferromagnetism is an intrinsic property of the $Cu^{II}-Gd^{III}$ couple irrespective of the degree of nuclearity and nature of the bridging ligand has been questioned by Costes et al. who recently reported on the first magnetostructurally characterized examples of discrete μ-phenolato-μ-oximato bridged, dinuclear $[Cu^{II}-Gd^{III}]$[13] and trinuclear $[Cu^{II}-Gd^{III}-Cu^{II}]$[6] species showing weak antiferromagnetism. These results point out the need for more experimental/theoretical studies about this heterometallic system in order to get a clear answer on the nature and pathway of the magnetic coupling which is involved.

Acknowledgment. This work was supported by the INTAS (Project 95-118) and the TMR Programme from the European Union (Contract ERBFMRXCT98-0181). Gratitude is expressed to Mr. Bruno Donadieu (Laboratoire de Chimie de Coordination du CNRS, Toulouse) for helpful assistance in using a Stoe image plate diffraction system.

Supporting Information Available: X-ray crystallographic files in CIF format. This material is available free of charge via the Internet at http://pubs.acs.org.

IC0110777

(29) Guillou, O.; Oushoorn, R. L.; Kahn, O.; Boubekeur, K.; Batail, P. *Inorg. Chim. Acta* **1992**, *198*−*200*, 119−131.